ELSEVIER

Journal of Power Sources 68 (1997) 153–158

JOURNAL OF POWER SOURCES

Structural stability of $LiMn_2O_4$ electrodes for lithium batteries [1]

M.M. Thackeray [a,*], M.F. Mansuetto [a], J.B. Bates [b]

[a] *Electrochemical Technology Program, Chemical Technology Division, Argonne National Laboratory, Argonne, IL 60 439, USA*

[b] *Solid State Division, Oak Ridge National Laboratory, Oak Ridge, TN 37 831, USA*

Accepted 14 October 1996

Abstract

The structural stability of $LiMn_2O_4$, which is of interest as an insertion electrode for rechargeable lithium batteries, is discussed with respect to processing techniques, composition, Li–Mn–O phase diagram, and electrochemical behavior. Particular attention is paid to processing conditions that result in the formation of lithium–manganese–oxide spinel products in which Mn^{2+} ions partially occupy the tetrahedral sites of the spinel structure. The electrochemical behavior of electron-beam and r.f. magnetron sputtered thin-film electrodes suggests the existence of partially inverse $Li_{1-x}Mn_2O_4$ spinel structures during an initial charge to 5.3 V. © 1997 Published by Elsevier Science S.A.

Keywords: Lithium batteries; Manganese oxides; Electrodes

1. Introduction

Lithium-ion cells that operate between 3 and 4 V are gaining increasing popularity for powering electronic equipment such as cellular phones, camcorders, and laptop computers [1]. Commercial cells currently contain a carbon anode, a liquid electrolyte consisting of a lithium salt dissolved in an organic solvent, and a $LiCoO_2$ cathode. Because of the relatively high cost of cobalt, considerable effort is being made to develop other suitable cathode materials. The spinel $Li[Mn_2]O_4$ provides an attractive alternative because it is a low-cost, environmentally acceptable material [2–5]. Unfortunately, a wide range of solid solution exists in the Li–Mn–O spinel system, which makes it difficult to fabricate an electrode with an exact, predetermined composition [6–8]. When the electrode has the ideal, normal spinel distribution of cations, $Li[Mn_2]O_4$, the Li ions occupy the tetrahedral sites (8*a*) of the spinel structure (space group $Fd3m$), and the Mn ions, the octahedral sites (16*d*). A Li/liquid electrolyte/$Li_x[Mn_2]O_4$ cell operates at approximately 4 V over the range $0 < x \leq 1$, and at approximately 3 V over the range $1 \leq x \leq 2$. Over the 4 V range, Li ions occupy the 8*a* tetrahedral sites, and over the 3 V range, predominantly the 16*c* octahedral sites. The 1 V drop reflects the difference in energy between the spinel-related phase, $Li_{1-x}Mn_2O_4$, and the rock-salt-related phase, $Li_{1+x}Mn_2O_4$.

It has recently been reported that all-solid-state lithium/lithium–phosphorus–oxynitride (Lipon)/$LiMn_2O_4$ cells, in which the $LiMn_2O_4$ electrode is fabricated in thin-film form by electron-beam (e-beam) evaporation or r.f. magnetron sputtering, can deliver an appreciable amount of capacity above 4 V [9,10]. On charge, these cells show a voltage plateau at 5 V, in addition to the expected voltage plateau at 4 V. In some instances, a voltage plateau at 4.6 V is observed during the initial charge to 5.3 V. The upper stability limit of the Lipon solid electrolyte is ≥ 5.5 V.

Because a wide range of solid solution exists within the Li–Mn–O family of spinel compounds, and because the composition of the spinel electrode plays a pivotal role in controlling the rechargeability of the electrode, careful process control is essential when synthesizing these electrodes at elevated temperatures. In this paper, the structural stability of $LiMn_2O_4$ is discussed in relation to processing techniques, reaction temperature, and electrochemical performance. An attempt has been made to interpret the electrochemical behavior of thin-film $LiMn_2O_4$ electrodes in terms of the cation distribution in electrode structures prepared by e-beam evaporation and r.f. magnetron sputtering.

2. Experimental

$LiMn_2O_4$ was synthesized by reaction of thoroughly blended powders of LiOH and chemically prepared manga-

* Corresponding author.

[1] This paper has been authored by a contractor of the US Government under contract No. W-31-109-ENG-38. Accordingly, the US Government retains a nonexclusive, royalty-free license to publish or reproduce the published form of this contribution, or allow others to do so, for US Government purposes.

PII S0378-7753(96)02624-9

nese dioxide (CMD) at 750 °C. X-ray data were collected on a Siemens D-5000 diffractometer with graphite monochromated Cu Kα radiation. High-temperature X-ray diffraction (XRD) patterns of samples were collected on a Pt/Rh heating strip, in air, with a Buhler HDK S1 high-temperature attachment. Samples were heated at 20 °C intervals and held at each temperature for 15 min prior to data collection. XRD patterns were recorded at a scan rate of 1.44 °C/min between 15 and 80° (2θ). Lattice constants were determined by least-squares refinement of the peak positions in the powder XRD patterns.

The electrochemical data were obtained from thin-film $LiMn_2O_4$ samples prepared by e-beam evaporation and r.f. magnetron sputtering. These data were provided by Oak Ridge National Laboratory. Detailed descriptions of electrode preparation, cell fabrication, and cell testing have been given elsewhere [9,10].

3. Results and discussion

3.1. Thermal stability of $LiMn_2O_4$

The XRD patterns of a heated $LiMn_2O_4$ sample show that several phase changes occur between room temperature and 1200 °C (Fig. 1). These results are consistent with previously reported thermogravimetric analysis (TGA) data and differential thermal analysis (DTA) data, which show the onset of distinct processes at approximately 780, 915, and 1060 °C [5,11]. These combined data provide evidence of the following reaction sequence:

(i) *780–915 °C (surface reaction)*

$$LiMn_2O_4 \rightarrow \delta Li_2MnO_3 + Li_{1-2\delta}Mn_{2-\delta}O_{4-3\delta-\delta'} + \delta'/2O_2 \quad (1)$$

During this reaction, oxygen is lost from $LiMn_2O_4$ and lithium diffuses to the particle surface, resulting in a disproportionation of $LiMn_2O_4$ into a tetragonal spinel phase, $Li_{1-2\delta}Mn_{2-\delta}O_{4-3\delta-\delta'}$, and a stable rock-salt phase, Li_2MnO_3. The tetragonal phase, in which the manganese oxidation state is less than 3.5, manifests itself in the XRD pattern at 840 °C by the splitting of the [311] peak of the cubic $LiMn_2O_4$ phase into the [311] and [113] peaks of the tetragonal phase (Fig. 1). The extent of the tetragonal (Jahn–Teller) distortion depends on the amount of oxygen lost from the sample and on the concentration of Mn^{3+} cations on the octahedral sites of the spinel structure [6]; at 840 °C, the c/a ratio of the tetragonal phase is 1.02, indicative of only a small deviation from ideal cubic symmetry ($c/a = 1.00$).

Note that in Eq. (1), no Li_2O is lost from the sample because it is contained by the Li_2MnO_3 phase on the particle surface. Note also that the tetragonal phase need not be an oxygen-deficient spinel phase, $LiMn_2O_{4-\delta}$, as reported by Tarascon et al. [4] and Yamada et al. [5]; it could, in principle, be a stoichiometric spinel phase that lies on the tie-line between $LiMn_2O_4$ and Mn_3O_4 in the Li–Mn–O phase diagram, designated $Li_{1-\delta}Mn_2O_{4-4/3\delta}$ in Fig. 2.

(ii) *≥915 °C*

Previously reported TGA and DTA data have shown the onset of a reversible phase transition at 915 °C [11], which is accompanied by a rapid loss of oxygen. The XRD data in Fig. 1 indicate that this phase transition can be attributed to the formation of a $LiMnO_2$ phase; it is formed at the expense of the Li_2MnO_3 rock-salt phase, which reacts with some of the tetragonal spinel phase. In an ideal simplified case, the reaction between the rock-salt phase and the spinel phase can be represented by

$$Li_2MnO_3 + LiMn_2O_4 \rightarrow 3LiMnO_2 + 1/2O_2 \quad (2)$$

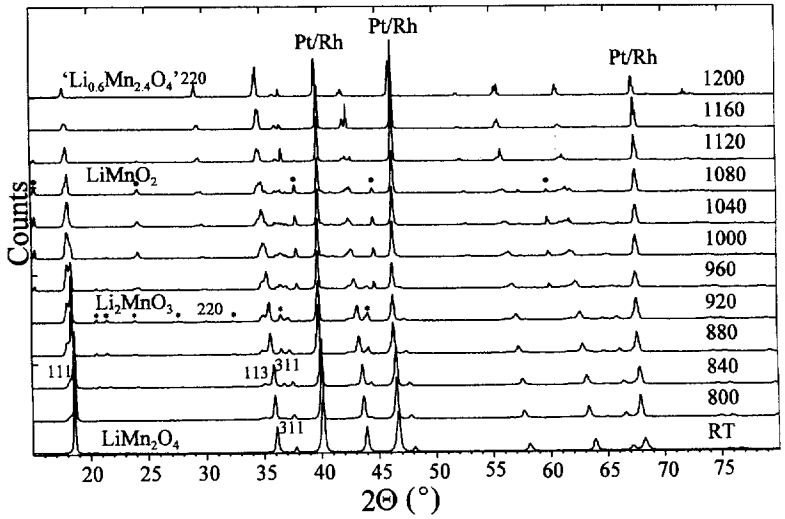

Fig. 1. XRD patterns of $LiMn_2O_4$ recorded in situ, from room temperature (RT) to 1200 °C. Characteristic peaks of (*) Li_2MnO_3 and (●) $LiMnO_2$ are indicated at 920 and 1200 °C, respectively.

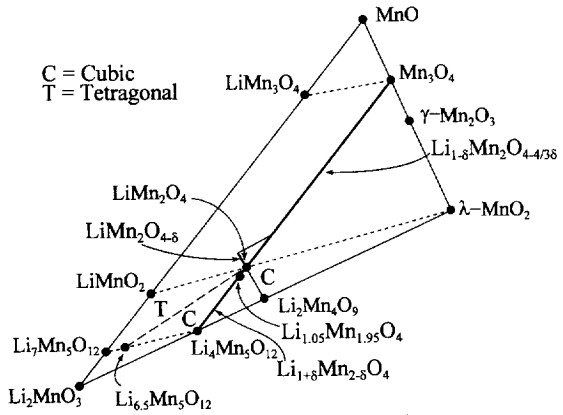

Fig. 2. Section of the Li–Mn–O phase diagram.

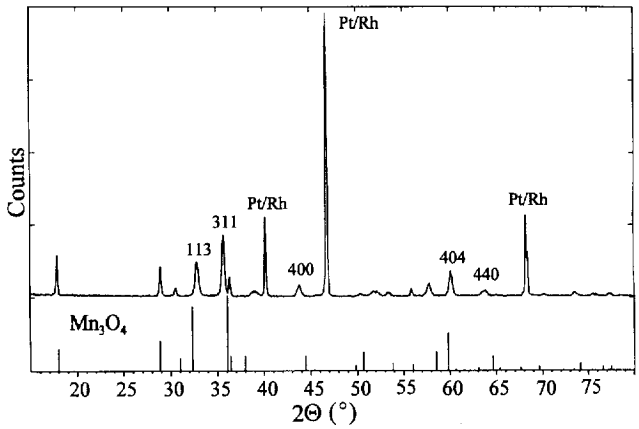

Fig. 3. XRD pattern of tetragonal $Li_{0.6}Mn_{2.4}O_4$. The calculated pattern of Mn_3O_4 is given below for comparison.

The $LiMnO_2$ phase exists to approximately 1120 °C, after which it recombines with the residual spinel phase to yield a single-phase (spinel) product.

(iii) *1060 °C*

The transition that was observed at 1060 °C for previously reported DTA and TGA data has been attributed to a reversible transition of a tetragonal spinel phase to cubic symmetry [11]. This transition was confirmed by the powder XRD pattern of the sample after rapid cooling to room temperature. At 1200 °C, the pattern could be indexed to a cubic unit cell with $a = 8.61(1)$ Å (Fig. 1), whereas after cooling the compound had tetragonal symmetry, with $c/a = 1.12$ (Fig. 3). This behavior is similar to that observed with Mn_3O_4, which transforms from tetragonal ($c/a = 1.16$ at room temperature) to cubic symmetry ($c/a = 1.00$) at 1160 °C [12]. The c/a ratios of various spinel-related phases, such as $Li_2Mn_2O_4$ ($c/a = 1.16$) [13], Mn_3O_4 ($c/a = 1.16$) [13], $Li_5Mn_4O_9$ ($c/a = 1.14$) [6], and $Li_7Mn_5O_{12}$ ($c/a = 1.11$) [6], were compared with the concentration of Mn^{3+} ions on the octahedral sites. This comparison indicated that a c/a ratio of 1.12 corresponds to the composition $(Li_{0.6}Mn_{0.4})_{tet}[Mn_2]_{oct}O_4$. Because Mn^{2+} ions have a stronger preference than Mn^{3+} and Mn^{4+} for tetrahedral sites, it is believed that the valence distribution of the cations in $Li_{0.6}Mn_{2.4}O_4$ is $(Li_{0.6}{}^{1+}Mn_{0.4}{}^{2+})_{tet}[Mn_2{}^{4+/3+}]_{oct}O_4$, with the Mn ions on the $[Mn_2]O_4$ subarray having an average oxidation state of 3.3.

The transition of $LiMn_2O_4$ from cubic to tetragonal symmetry requires the loss of both lithium and oxygen. If the final product is assumed to be a spinel that falls on the $LiMn_2O_4$–Mn_3O_4 tie line (Fig. 2), the overall reaction at 1200 °C is given by

$$LiMn_2O_4 \rightarrow Li_{1-\delta}Mn_2O_{4-4/3\delta} + \delta/2Li_2O + 5\delta/12O_2 \quad (3)$$

At elevated temperatures, Mn ions replace Li^+ ions on the tetrahedral sites of the spinel structure; if all the lithium were replaced, the product would be Mn_3O_4 at $\delta = 1$. These high temperature data, therefore, provide evidence of lithium–manganese–oxide spinels with Mn^{2+}, Mn^{3+}, and Mn^{4+} cations within a single close-packed oxygen array.

3.1.1. $LiMn_2O_4$ electrodes deposited by e-beam evaporation or r.f. magnetron sputtering

The $LiMn_2O_4$ electrodes that were deposited by e-beam evaporation or r.f. magnetron sputtering had electrochemical charge/discharge profiles that were significantly different from profiles that are normally observed with powder $LiMn_2O_4$ samples in liquid electrolyte cells (Fig. 4(a)–(d)) [9,10]. A typical voltage profile for a Li/liquid electrolyte/$LiMn_2O_4$ cell is given in Fig. 4(a); it shows a two-step reaction at approximately 4 V, which is associated with the insertion of lithium into tetrahedral sites of the spinel structure, and a voltage plateau at approximately 3 V, which is associated with the insertion of lithium into octahedral sites. By contrast, the voltage profiles obtained from three separate Li/Lipon/$LiMn_2O_4$ cells (Fig. 4(b)–(d)) show processes that occur between 2.2 and 5 V [10].

Fig. 4(b)–(d) shows that Li/Lipon/$LiMn_2O_4$ cells deliver approximately one-half of their capacity below 3 V. These data are consistent with a spinel-electrode composition $LiMn_2O_4$. Moreover, the XRD patterns of e-beam and r.f.-sputtered $LiMn_2O_4$ electrodes are, in general, characteristic of a cubic, single-phase spinel product with a lattice parameter $8.16\ \text{Å} \leq a \leq 8.20\ \text{Å}$ [10], which is slightly smaller than that of the stoichiometric 'normal' spinel $Li[Mn_2]O_4$ (8.24 Å) [13]. The voltage drop between 2.8 and 2.1 V that is observed in Fig. 4(b)–(d) can be attributed to a polarization effect; it is associated with the diffusion of lithium across the interface that separates the tetragonal $Li_{1+x}Mn_2O_4$ spinel phase on the surface of the film from the unreacted, cubic $LiMn_2O_4$ phase below the surface. The voltage of the cell on open circuit relaxes to the expected 3 V for the two-phase electrode, as shown in Fig. 4(b).

Of particular interest to this study are the voltage profiles of the charge and discharge processes that occur above 3 V. These profiles can vary significantly from one electrode to another; they indicate that the cations in thin-film $LiMn_2O_4$ electrodes are distributed in arrangements that differ from the 'normal' distribution of cations in $Li[Mn_2]O_4$. If some Mn ions are permitted to occupy either the tetrahedral 8*a* or interstitial 16*c* sites of the spinel, then, in principle, it would be

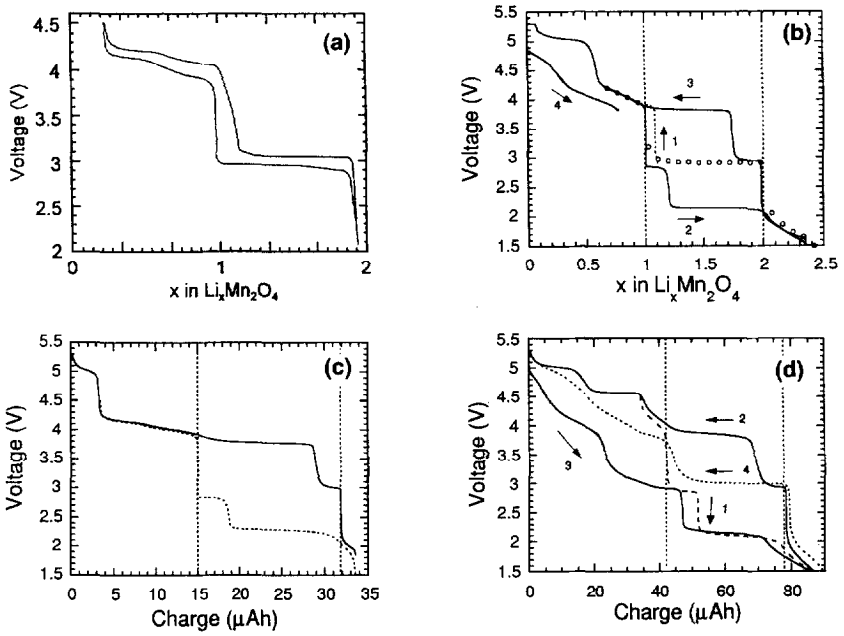

Fig. 4. Electrochemical charge/discharge profiles of: (a) standard Li/$LiMn_2O_4$ liquid electrolyte cell (i=0.2 mA), and (b)–(d) three Li/Lipon/$LiMn_2O_4$ cells (i=0.2 μA): (b), (c) e-beam evaporated $LiMn_2O_4$ and (d) r.f. magnetron sputtered $LiMn_2O_4$. Small circles in (b) are open-circuit voltage readings [10]. Numbers in (b) and (d) indicate the sequence of the charge/discharge processes.

possible for stoichiometric $LiMn_2O_4$ to adopt the following configurations.

(i) Model I:

$(Li_{1-x}Mn_x)_{8a}[Li_xMn_{2-x}]_{16d}O_4 \quad (0<x\leqslant 0.5)$

This configuration has a partial inversion of the spinel structure, in which Mn^{2+} ions occupy the tetrahedral sites. Note that the end member (at $x=0.5$) has the formulation $(Li_{0.5}Mn_{0.5}{}^{2+})_{8a}[Li_{0.5}Mn_{1.5}{}^{4+}]_{16d}O_4$, in which the Mn ions on the octahedral sites are all tetravalent.

(ii) Model II:

$(Li_{1-x-y})_{8a}\{Mn_xLi_y\square_{2-x}\}_{16c}[Li_xMn_{2-x}]_{16d}O_4$

$(0<x\leqslant 0.5,\ 0\leqslant y\leqslant x)$

In this configuration, a fraction of the Mn ions partially occupy the interstitial octahedral 16*c* sites of the spinel structure (□ refers to a vacancy). All the Mn ions reside in edge-shared MnO_6 octahedra, as they do in $Li[Mn_2]O_4$; they are of mixed $Mn^{4+/3+}$ valence. The presence of Mn in the 16*c* sites destabilizes the tetrahedral 8*a* sites. Although the simultaneous occupation of the 8*a* tetrahedra and 16*c* octahedra (which share faces with one another) by lithium and manganese may seem unlikely and energetically unfavorable, neutron diffraction data indicate that in the lithiated spinel $Li_2[Mn_2]O_4$, the Li ions are distributed over both sets of sites [14]. It is, therefore, postulated that metastable Model II-type compounds occur with some Mn on the 16*c* sites, particularly when the compounds are fabricated under uncontrolled sputtering conditions. With such an arrangement of cations, a small fraction of Li ions on the tetrahedral sites is expected to be displaced into neighboring octahedral sites to minimize Li–Mn electrostatic interactions.

No satisfactory explanation for the electrochemical behavior of $LiMn_2O_4$ electrodes in Fig. 4(b)–(d) could be found solely in terms of Model I-type structures. On the other hand, Model II-type structures do offer a possible explanation. In the interpretation of the voltage profiles in Fig. 4(b)–(d) that follows, the relative amounts of lithium that were inserted into, or extracted from, the $LiMn_2O_4$ structures were determined from the capacities delivered over selected compositional ranges.

For example, the voltage profile in Fig. 4(c) can be interpreted in terms of a cation distribution in which $x=0.1$

$(Li_{0.90-y})_{8a}\{Li_yMn_{0.10}\square_{1.80}\}_{16c}[Li_{0.10}Mn_{1.90}]_{16d}O_4$

$(y\approx x)$

During the initial charge to 5.3 V, 0.8 Li^+ ions are removed from the tetrahedral sites over the voltage range 3.9 to 4.2 V. The Mn^{3+} ions on the 16*c*–16*d* subarray of the spinel structure are oxidized to Mn^{4+} and are not displaced during the extraction of lithium. The small inflection on the electrochemical curve when one-half of the lithium has been extracted from the tetrahedral sites is consistent with an ordering process on the 8*a* tetrahedra, also observed in $Li_{1-x}[Mn_2]O_4$ at $x\approx 0.5$ [2]. The remaining 0.2 Li^+ ions are extracted at 5 V from octahedral sites; this is consistent with the voltage that was necessary to extract lithium from the octahedral sites of the spinel $V[LiNi]O_4$ [15]. With this interpretation, the final MnO_2 product in Fig. 4(a) would have the cation distribution $\{Mn_{0.1}\square_{1.9}\}_{16c}[Mn_{1.9}\square_{0.1}]_{16d}O_4$.

Fig. 4(b) can be interpreted in terms of a Model II configuration with $x=0.3$, i.e., with the cation distribution

$(Li_{0.7-y})_{8a}\{Li_yMn_{0.3}\square_{1.4}\}_{16c}[Li_{0.3}Mn_{1.7}]_{16d}O_4 \quad (y\approx x)$

The single-phase reaction process that occurs on charge between 3.9 and 4.3 V can be attributed to the extraction of

0.4 Li^+ ions from the tetrahedral 8*a* sites. The remaining Li ions are extracted from the 16*c* and 16*d* octahedral sites at 5 V. The relatively flat voltage profile at 5 V indicates that extraction of lithium from the crystallographically independent 16*c* and 16*d* sites cannot be readily distinguished during the first charge, consistent with Fig. 4(c). If the Mn_2O_4 subarray remains intact during lithium extraction, then the resulting MnO_2 defect rock-salt phase would have the cation distribution $\{Mn_{0.3}\square_{1.7}\}_{16c}[Mn_{1.7}\square_{0.3}]_{16d}O_4$ at the top of charge. The subsequent discharge from 5.3 to 3.9 V indicates a two-stage reaction during which lithium is believed, first, to occupy octahedral sites (predominantly the 16*d* sites) and thereafter to partially fill the 8*a* tetrahedral sites.

The initial charge to 5.3 V in Fig. 4(d) shows, unlike Fig. 4(b) and (c), a two-phase reaction at 4.6 V. It is proposed that the presence of the 4.6 V plateau arises from a Model II-type structure, and that a critically high concentration of Mn^{3+} occurs on the 16*c* sites, at least in some localized regions (clusters) of the thin-film electrode (which could affect the crystal symmetry of localized regions [2]). It is proposed that the high concentration of Mn^{3+} ions on the octahedral 16*c* sites could nucleate the following disproportionation (internal redox) reaction at 4.6 V

$$2Mn^{3+}_{16d,16c} \rightarrow Mn^{4+}_{16d} + Mn^{2+}_{8a} \quad (4)$$

during which Mn^{2+} ions migrate into tetrahedral 8*a* sites to generate a partially inverse defect spinel structure. (It is possible that some tetrahedral Mn^{2+} ions may act as nucleating agents for the disproportionation reaction.) This is analogous to the situation that occurs when lithium is extracted from lithiated hausmannite $(LiMn)_{16c}[Mn_2]_{16d}O_4$ [13] to generate the spinel phase, hausmannite, $Mn[Mn_2]O_4$

$$3Mn^{2.33+}_{16c,16d} \rightarrow 2Mn^{3+}_{16d} + Mn^{2+}_{8a} \quad (5)$$

With this hypothesis, the voltage profile in Fig. 4(d) could be interpreted in terms of a Model II-type $LiMn_2O_4$ electrode

$$(Li_{0.60-y})_{8a}\{Li_yMn_{0.40}\square_{1.2}\}_{16c}[Li_{0.40}Mn_{1.6}]_{16d}O_4 \quad (y \approx x)$$

in which $x_{average} \approx 0.4$, but with x_{max} probably > 0.4 in some localized regions of the structure to nucleate the disproportionation reaction.

In Fig. 4(d), from 3.9 to 4.6 V, 0.2 Li^+ ions are initially removed from the tetrahedral 8*a* sites, with a concomitant oxidation of Mn^{3+} to Mn^{4+} on the 16*c* and 16*d* sites. At the composition $Li_{0.8}Mn_2O_4$, the average manganese oxidation state is 3.6. Further removal of lithium from the structure at 4.6 V is associated with the onset of the disproportionation reaction, which generates the partially inverse defect spinel phase $(Li_{0.40}Mn_{0.40}\square_{0.2})_{8a}[Li_{0.40}Mn_{1.60}]_{16d}O_4$. In this $Li_{0.8}Mn_2O_4$ spinel phase all the Mn ions on the tetrahedral sites are divalent, and all the Mn ions on the octahedral sites are tetravalent. Further extraction of lithium from the defect spinel phase necessitates the oxidation of the Mn^{2+} ions on the tetrahedral sites. This process causes a cooperative displacement of the tetrahedrally coordinated Mn ions back into the 16*c* sites of the 16*c*–16*d* subarray because of the strong octahedral-site preference of the Mn^{3+} ion. The result is a two-phase electrode consisting of the defect spinel phase and a defect rock-salt phase. It is evident from Fig. 4(d) that the two-phase region is associated with the removal of 0.4 Li^+ ions from the structure; in this case, the end members of the two-phase region would be $(Li_{0.40}Mn_{0.40}\square_{0.2})_{8a}[Li_{0.40}Mn_{1.60}]_{16d}O_4$ (defect spinel) and $\{Mn_{0.4}Li_\delta\square_{1.6-\delta}\}_{16c}[Li_{0.4-\delta}Mn_{1.60}\square_\delta]_{16d}O_4$ (defect rock-salt). Extraction of the remaining 0.4 Li^+ ions from the octahedral sites takes place at 5 V, consistent with the interpretation given for Fig. 4(b) and 4(c). With this interpretation, the MnO_2 defect rock-salt phase that is formed at the top of charge would have the distribution $\{Mn_{0.4}\square_{1.6}\}_{16c}[\square_{0.40}Mn_{1.60}]_{16d}O_4$.

Of particular significance is the profile of the subsequent discharge from 5.3 to 2.8 V in Fig. 4(d). The two-phase region observed at 4.6 V on charge does not occur on discharge; this finding indicates that lithium insertion does not regenerate the partially inverse spinel structure. Instead, the shape of the discharge profile is consistent with lithium insertion into a defect rock-salt MnO_2 phase; the reaction takes place in three discrete single-phase processes, associated with the lithium occupation of: (i) octahedral sites (predominantly 16*d*) between 5.0 and 4.2 V: (ii) 8*a* tetrahedral sites between 4.2 and 3.9 V, and (iii) octahedral sites (predominantly 16*c*) between 3.9 and 2.9 V. Further insertion of lithium reduces the Mn ions below an average oxidation state of 3.5. The onset of a Jahn–Teller effect results in a two-phase electrode consisting of a cubic $LiMn_2O_4$ phase and a tetragonal $Li_2Mn_2O_4$ phase. Assuming that the $[Li_{0.4}Mn_{1.6}]O_4$ spinel framework remains intact during lithium insertion and extraction, the tetragonal phase would have the cation distribution $\{Mn_{0.4}Li_{1.6}\}_{16c}[Li_{0.4}Mn_{1.6}]_{16d}O_4$. On the second charge to 5.3 V (curve 4 in Fig. 4(d)), the voltage profile does not show the onset of a two-phase reaction at 4.6 V, but rather has a shape which is closer to that of the previous discharge. Such behavior is expected if the Mn ions outside the $[Li_{0.4}Mn_{1.6}]O_4$ framework in the initial structure become randomly distributed over the 16*c* octahedral sites of the spinel structure during the first charge on the 4.6 V plateau, when the Mn ions move from their initial localized 16*c* positions to 8*a* sites and then back to 16*c* sites. On the second charge, therefore, no nucleation centers (regions of high manganese concentration) are left to aid the disproportionation reaction, so the electrode adopts a predominant defect rock-salt structure in which the Mn ions remain fixed in their octahedral sites. Note that in this model of $LiMn_2O_4$, the Mn ions occupy only 20% of the available 16*c* sites, and that there exists an energetically favorable 16*c*–8*a* pathway for Mn diffusion during lithium extraction from the structure. By contrast, the concentration of Mn on the 16*d* sites is too high for these ions to move into neighboring, energetically unfa-

[2] Indeed, some e-beam and sputtered $LiMn_2O_4$ samples that show the 4.6 V plateau give XRD patterns with split [111] and [311] reflections, indicating either a phase with reduced symmetry or possibly two cubic phases.

vorable, tetrahedral (8*b*) sites; this is a factor that contributes to the well-known stability of the $[Mn_{2-x}Li_x]_{16d}O_4$ spinel framework to lithium insertion and extraction reactions [6,13].

In conclusion, the results suggest the existence of partially inverse $Li_{1-x}Mn_2O_4$ spinel structures during an initial charge to 5.3 V of thin-film $LiMn_2O_4$ electrodes prepared by e-beam evaporation and r.f. magnetron sputtering. It is worthwhile to point out that an electrochemical process at ~4.5 V has also been detected, to a very minor degree, in Li–Mn–O spinel electrodes prepared by conventional solid-state reactions. Thus, even in powder electrodes, a deviation from the ideal normal spinel distribution of cations in $Li[Mn_2]O_4$ is possible [4,16]. Moreover, recent analyses of the XRD patterns of $LiMn_2O_4$ powders (preparation temperature = 750 °C) have shown insignificant scattering from Mn ions on the tetrahedral sites [16], consistent with a Model II-type structure. Nevertheless, further work is required to test the interpretation provided in this paper and to gain a greater understanding of the reaction processes occurring in high-voltage (>4 V) $LiMn_2O_4$ electrodes.

Acknowledgements

Professor John B. Goodenough is thanked for reviewing the paper and for suggesting the possibility that tetrahedral-site Mn^{2+} ions might be required to aid the disproportionation reaction.

References

[1] S. Megahed and B. Scrosati, *J. Power Sources, 51* (1994) 79.
[2] T. Ohzuku, M. Kitagawa and T. Hirai, *J. Electrochem. Soc., 137* (1990) 769.
[3] J.M. Tarascon, E. Wang, F.K. Shokoohi, W.R. McKinnon and S. Colson, *J. Electrochem. Soc., 138* (1991) 2859.
[4] J.M. Tarascon, W.R. McKinnon, F. Coowar, T.N. Bowmer, G. Amatucci and D. Guyomard, *J. Electrochem. Soc., 141* (1994) 1421.
[5] A. Yamada, K. Miura, K. Hinokuma and M. Tanaka, *J. Electrochem. Soc., 142* (1995) 2149.
[6] M.M. Thackeray, A. De Kock, M.H. Rossouw, D.C. Liles, D. Hoge and R. Bittihn, *J. Electrochem. Soc., 139* (1992) 363.
[7] R.J. Gummow, A. De Kock and M.M. Thackeray, *Solid State Ionics, 69* (1994) 59.
[8] Y. Gao and J.R. Dahn, *Appl. Phys. Lett., 66*(19) (1995) 2487.
[9] J.B. Bates, D. Lubben, N.J. Dudney and F.X. Hart, *J. Electrochem. Soc., 142* (1995) L149.
[10] J.B. Bates, D. Lubben, N.J. Dudney, R.A. Zuhr and F.X. Hart, *Proc. 188th Meet.The Electrochemical Society, Chicago, Il, USA, 8–13 Oct. 1995,* in press.
[11] M.M. Thackeray and M.F. Mansuetto, *Mater. Res. Bull., 31* (1996) 133.
[12] M. Keller and R. Dieckmann, *Ber. Bunsenges. Phys. Chem., 89* (1985) 1095.
[13] M.M. Thackeray, W.I.F. David, P.G. Bruce and J.B. Goodenough, *Mater. Res. Bull., 18* (1983) 461.
[14] W.I.F. David, M.M. Thackeray, L.A. de Picciotto and J.B. Goodenough, *J. Solid State Chem., 67* (1987) 316.
[15] G.T.-K. Fey, W. Li and J.R. Dahn, *J. Electrochem. Soc., 141* (1994) 2279.
[16] Y. Gao and J.R. Dahn, *J. Electrochem. Soc., 143* (1996) 100.